International Journal of Physical Sciences and Engineering
Available online at www.sciencescholar.us
Vol. 6 No. 1, April 2022, pages: 1-8
e-ISSN : 2550-6943, p-ISSN : 2550-6951
https://doi.org/10.53730/ijpse.v6n1.2940

Temporal Analysis on Spectral Reflectance of Clove Vegetation Based on Landsat 8 Imagery

I Made Yuliara [a], **Ni Nyoman Ratini** [b], **I Gde Antha Kasmawan** [c]

Manuscript submitted: 27 November 2021, Manuscript revised: 18 December 2021, Accepted for publication: 05 January 2022

Corresponding Author [a]

Keywords

clove vegetation;
Buleleng Regency;
Landsat 8;
spectral reflectance;
temporal analysis;

Abstract

This study aims to analyze temporally the spectral reflectance of clove vegetation using Landsat 8 multitemporal imagery data in Buleleng district, Bali. The analysis method uses the conversion of raw data from Landsat 8 images to the spectral reflectance value at the Top of Atmosphere (TOA). This conversion scales back the pixel values of the Landsat 8 image in the visible spectrum, namely bands 2, 3, 4, and infrared bands 5, 6, and 7 into percentage units. The temporal analysis technique is carried out by grouping the time series of Landsat 8 image data for 1 period, in 2015, into 4 quarterly groups based on the acquisition time, namely Quarter I (January, February, March), Quarter II (April, May, June), Quarter III (July, August, September) and Quarter IV (October, November, December). The results showed that the graph pattern of the average percentage of spectral reflectance in each quarter was the same and in the infrared spectrum was greater than the visible spectrum. The average value of the largest spectral reflectance was found in the second Quarter which was acquired by band 5 of 28.143%, while the smallest in the first Quarter which was acquired by band 2 was 2.503%.

Contents

[a] Udayana University, Denpasar, Indonesia
[b] Udayana University, Denpasar, Indonesia
[c] Udayana University, Denpasar, Indonesia

1 Introduction

The spectral reflectance of an object is an object feature that is expressed as the ratio of the reflected energy to the energy incident on the object's surface which is measured as a function of wavelength (Rees, 2013). The sensitivity of several sensors owned by remote sensing satellite systems to the spectral response due to changes in land cover on earth, both vegetative and non-vegetative, is used as the basis for the formation of remote sensing data (Abd El-Kawy et al., 2011; Chen et al., 2013; Green et al., 2000). The value of the spectral reflectance in satellite images is represented by the value of pixels in satellite images (Lillesand et al., 2015; Rees, 2013). The vegetative phase (development or growth) and the generative phase (production period) of a vegetation object will provide different spectral response features when the reflectance is captured by the sensor in a remote sensing system. Clove trees or vegetation for 1 period (1 year) in the vegetative phase, gives the appearance of a more dominant green color, while in the generative phase (when flowering is ready to be harvested), its appearance is relatively changing. The difference in appearance like this will give a different reflectance value when recorded by the remote sensing sensor. Changes or dynamics of the spectral reflectance response that occur can indicate that the physical condition of the vegetation object is changing such as growth, development or its condition is in the production period which can be monitored in real-time.

Many studies on spectral reflectance to assess and study the characteristics of objects on the earth's surface have been carried out. The study analyzed the spectral reflectance to characterize and differentiate Sago trees from other types of coconut (oil palm and nipa) and determine their implications for optical satellite imagery (Santillan & Makinano-Santillan, 2018). The analytical method used in this study is the average spectral reflectance curve of each species measured in the wavelength range 345 - 1045 nm using the USB4000-VIS-NIR Ocean Optic Mini Fiber Optic Spectrometer. The in-situ reflectance data obtained were resampled to match the spectral response of several satellite images, namely 4 bands of ALOS AVNIR-2 imagery, 3 bands of ASTER VNIR, 4 bands of Landsat 7 ETM+, 5 bands of Landsat 8, and 8 bands of Worldview-2 imagery. (WV2). The results of the analysis of this study indicate that the spectral reflectance at near-infrared wavelengths, particularly at 770, 800, and 875 nm, is the best wavelength at which sago palms can be distinguished from other trees (Sims & Gamon, 2002).

Research using temporal satellite imagery such as Landsat or other types of imagery is related to global-scale vegetation which correlates spectral reflectance with the greenness of vegetation (vegetation index) and can effectively monitor growth, vegetation development and predict chlorophyll concentration (Sims & Gamon, 2003; Broge & Mortensen, 2002). Besides, it is also used to determine plant biomass, map land drought, Leaf Area Index (LAI) to estimate productivity (Adams & Gillespie, 2006; Beeri et al., 2007; Green et al., 2000; Ozdogan, 2010; Xie et al., 2008). Research on the spectral reflectance of clove vegetation on visible waves (bands 2, 3, 4) and infrared (bands 5, 6, and 7) using Landsat 8 satellite imagery recorded on 26 May 2016 at path/row = 117/66 and 6 July 2016 at path/row = 116/66. The results of the analysis of the spectral response on the spectral reflectance curve produced an average spectral reflectance percentage of 66.08% in band 5 (Yuliara et al., 2017). Another study that links vegetation to rainfall extensively uses MODIS multitemporal imagery intending to know the sustainability of the agro-ecosystem (Wang et al., 2010).

From the description above, this study will analyze temporally the dynamics of the spectral reflectance pattern of clove vegetation by utilizing remote sensing satellite technology based on multitemporal Landsat 8 imagery data in the Buleleng district, Bali (Yuliara et al., 2018; Roy et al., 2016). Descriptive analysis was conducted to provide an assessment of the condition of clove vegetation for 1 year (1 period), namely 2015. The advantages of using Landsat 8 image data in this study are that apart from having a spatial resolution of 30 m, Landsat 8 image data is also available periodically and has a temporal resolution of 16 (Teixeira Pinto, 2020; Vermote et al., 2016; Storey et al.,).

2 Materials and Methods

This study uses multitemporal data from Landsat 8 imagery at coordinates 8° 03' 40'' – 8° 23' 00'' South Latitude and 114° 25' 55'' – 15° 27' 28'' East Longitude. The recording period is 1 year, namely 2015. All preprocessing and processing of image data use the Idrisi Terrset 18.21 image processor which includes rectification, masking, calibration of spectral radiance, and conversion of spectral reflectance on the Top of Atmosphere (TOA) with correction of the sun angle using the equation, namely (Teixeira Pinto, 2020):

$$\rho_\lambda = \frac{\rho'_\lambda}{\cos\theta_{SZ}} = \frac{\rho'_\lambda}{\sin\theta_{SE}} = \frac{M_\rho Q_{cal} + A_\rho}{\sin\theta_{SE}}$$

Where:

ρ'_λ = Value of spectral reflectance without correction for the angle of the sun
M_ρ = Band specific multiplicative rescaling factor, where x is the Band in REFLECTANCE_MULT_BAND_x
A_ρ = Band specific additive rescaling factor of metadata, where x is Band in REFLECTANCE_ADD_BAND_x
Q_{cal} = Quantized and calibrated standard product pixel values (DN)
θ_{SE} = Local sun elevation angle. The scene center sun elevation angle in degrees (SUN_ELEVATION).
θ_{SZ} = Local solar zenith angle; $\theta_{SZ} = 90° - \theta_{SE}$

To get a complete image of the study area, cropping is done to the image resulting from the mosaic of 2 image scenes. Improvements to the position of objects in the image are carried out by geometric correction referring to 9 Ground Control Points (GCPs) using the nearest neighbor method (Coondoo & Dinda, 2008). The position or coordinates of the clove vegetation in the image are identified through the results of measuring the coordinates of the clove vegetation in the field using the Global Positioning System (GPS) smartphone application (Myeong et al., 2006). The observation points whose clove vegetation coordinates were measured were chosen at locations with homogeneous clove vegetation distribution (Yuliara et al., 2020).

The technique of analyzing temporal data for Landsat 8 images is done by dividing multitemporal images for 1 year into 4 quarterly data groups based on data acquisition at the time of recording, namely: Quarter I data acquisition in January, February, and March, Quarter II acquisition in April, May, and June, Quarter III acquisition in July, August, September, and Quarter IV data acquisition in October, November, December. The grouping of data into quarters like this is also to adjust the reporting carried out by the Forestry and Plantation Service of the Buleleng Regency Government in 2015, namely regarding the area and production of plantations in Buleleng Regency (Dinas Kehutanan dan Perkebunan Pemkab Buleleng, 2015).

Landsat 8 image bands that were processed and analyzed in this study each series amounted to 6 bands, namely band 2 (B2), band 3 (B3), band 4 (B4) which is a visible electromagnetic wave spectrum with a wavelength, λ=0.450 to 0.680 μm and band 5 (B5), band 6 (B6), band 7 (B7) which is a spectrum of infrared electromagnetic waves with λ=0.650 to 0.885 μm. The data processing flow chart in this study is presented in Figure 1.

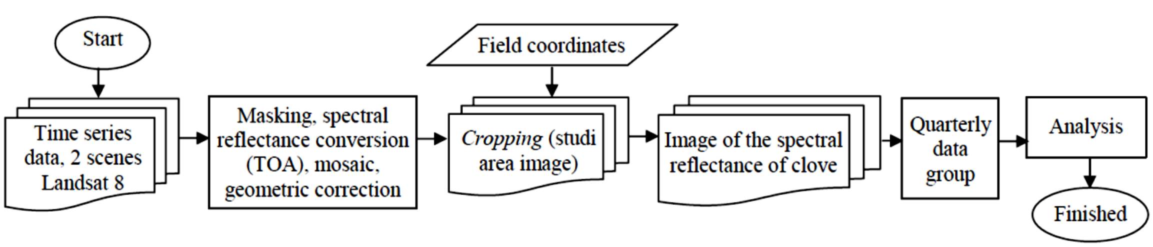

Figure 1. Research flow chart

3 Results and Discussions

The results of the spectral response obtained in this study are a function of wavelength which is represented by 6 bands from Landsat 8 imagery constructed from the reflection or emission of electromagnetic energy at different wavelengths as shown in Figure 2.

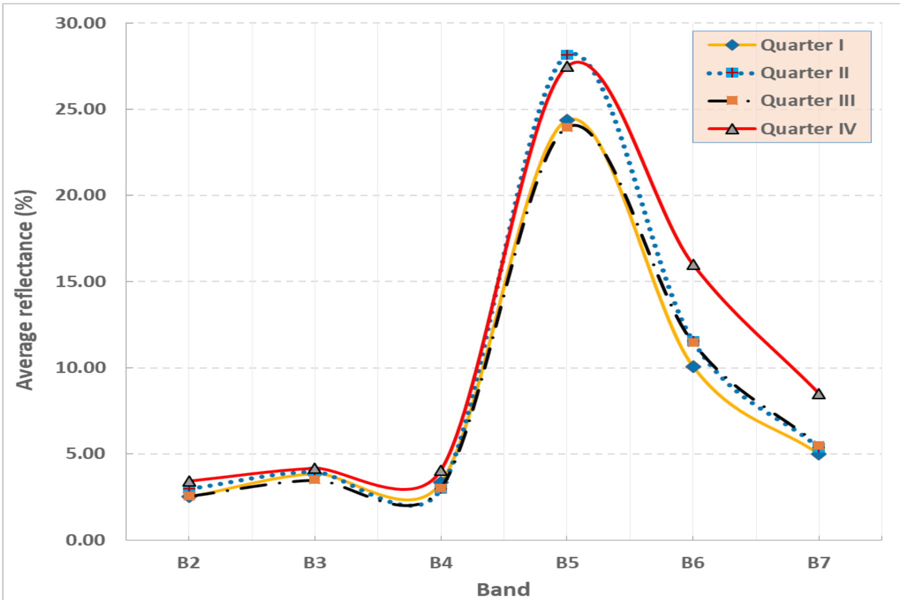

Figure 2. The average spectral reflectance of the 6 bands analyzed

The graph in Figure 2 shows that the percentage curve pattern of the average spectral reflectance every quarter produced shows the same curve pattern and has a unique shape. In the infrared spectrum (B5, B6, and B7), the average percentage of the spectral reflectance of clove vegetation shows a higher value than the visible spectrum (B2, B3, and B4). The highest percentage of the average spectral reflectance value is found in B5 which is the primary peak, while B3 is the secondary peak. This shows that at B5 the spectral reflectance of vegetation is detected to be greater than that of the other bands. In this condition, it can also be assumed that with healthy vegetation and dense canopy cover, the percentage of spectral reflectance is higher in the infrared spectrum than in the visible wave spectrum (Elachi & Van Zyl, 2021; Rees, 2013; Weng, 2011). The low spectral reflectance values in the visible spectrum (blue and red) are caused by vegetation absorbing a lot of energy that comes to the leaf surface which is used for photosynthesis. The amount of energy absorbed can reach 90% of the total energy that comes to the leaf surface of vegetation (Weng, 2011). Green vegetation has unique spectral reflectance characteristics which are influenced by leaf structure and composition such as chlorophyll, organic matter, water, leaf shape, and area (Huete & Glenn, 2011). The dynamics of the spectral reflectance values of cloves in each band are shown in Figure 3.

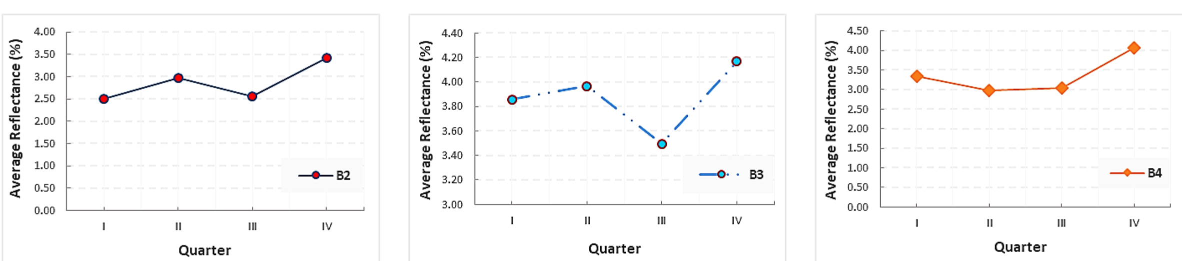

(a) (b) (c)

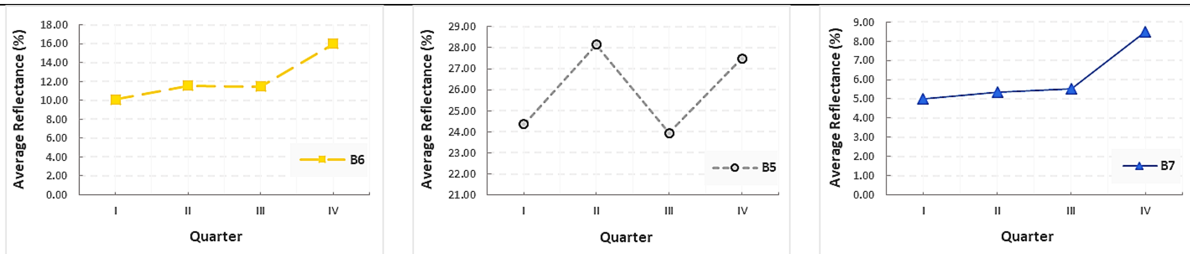

(d) (e) (f)

Figure 3. Average spectral reflectance from Quarter I to IV in each band

The average value of the largest spectral reflectance was in the second quarter which was acquired by image B5 as shown in Figure 3 (c), which was 28.143%, while the smallest was in the first quarter which was acquired by B2, Figure 3 (a), which was 2,503 %. The difference in the average value of the largest spectral reflectance from Quarter I to II is 3.774% and the smallest is 0.110%. The difference from the second to third quarters is the largest value is 4.205% and the smallest is 0.054%, while from the third to fourth quarters the largest value is 4.531% and the smallest is 0.673%. The dynamics of the average value of the spectral reflectance at each quarterly change indicates that there has been a change in the physical condition of the clove vegetation which can be interpreted as the clove vegetation being in the vegetative phase or the generative phase (Roth et al., 2019; Limin et al., 2015).

The curve pattern from a quarter I to II shows the spectral reflectance of all bands rising, except for B4. Band 4 (λ=0.630 to 0.680 m) from Quarter I to II shows that energy absorption at this wavelength is still quite high or the percentage of spectral reflectance is decreasing. This happens because the clove vegetation uses most of the wavelength fraction of band 4 that it comes to carry out for photosynthesis (Weng, 2011). The curve pattern from the second to third quarters shows that the spectral reflectance at B2, B3, and B5 decreased, while at B3, B6 and B7 there was a relatively significant increase. The fluctuation of the decrease in spectral reflectance is quite large, it can be assumed that in the third quarter the vegetation absorbs quite a lot of energy to go to the generative phase at which time the physical condition of the vegetation changes its appearance. It is presumed that the change in the spectral reflectance value is most likely caused by a change in the color of the clove flower. The curve pattern from the third to fourth quarters shows that the spectral reflectance of all bands has increased, which means that there is only a slight absorption of energy coming to the leaves/vegetation, a reduction in the photosynthesis process. Comprehensively, changes in the curve pattern from quarter to quarter obtained in this study have implications for the dynamics of spectral reflectance.

4 Conclusion

Based on the descriptive analysis of the results and discussion in this study, it can be concluded that, temporally, there has been a dynamic of the spectral reflectance pattern of clove vegetation for 1 period (1 year). This is indicated by changes in the pattern of the spectral reflectance curve from every quarter, where changes in the pattern of this spectral reflectance curve can be used as an indication that there has been a physical change in conditions in clove vegetation when it is in the vegetative and generative phases.

Acknowledgments
The authors would like to thank Udayana University for funding this research through the Leading Research Scheme from the Study Program, the year 2021.

References

Abd El-Kawy, O. R., Rød, J. K., Ismail, H. A., & Suliman, A. S. (2011). Land use and land cover change detection in the western Nile delta of Egypt using remote sensing data. *Applied geography*, *31*(2), 483-494. https://doi.org/10.1016/j.apgeog.2010.10.012

Adams, J. B., & Gillespie, A. R. (2006). *Remote sensing of landscapes with spectral images: A physical modeling approach*. Cambridge University Press.

Beeri, O., Phillips, R., Hendrickson, J., Frank, A. B., & Kronberg, S. (2007). Estimating forage quantity and quality using aerial hyperspectral imagery for northern mixed-grass prairie. *Remote Sensing of Environment*, *110*(2), 216-225. https://doi.org/10.1016/j.rse.2007.02.027

Broge, N. H., & Mortensen, J. V. (2002). Deriving green crop area index and canopy chlorophyll density of winter wheat from spectral reflectance data. *Remote sensing of environment*, *81*(1), 45-57. https://doi.org/10.1016/S0034-4257(01)00332-7

Chen, J., Lu, M., Chen, X., Chen, J., & Chen, L. (2013). A spectral gradient difference based approach for land cover change detection. *ISPRS journal of photogrammetry and remote sensing*, *85*, 1-12. https://doi.org/10.1016/j.isprsjprs.2013.07.009

Coondoo, D., & Dinda, S. (2008). Carbon dioxide emission and income: A temporal analysis of cross-country distributional patterns. *Ecological Economics*, *65*(2), 375-385. https://doi.org/10.1016/j.ecolecon.2007.07.001

Dinas Kehutanan dan Perkebunan Pemkab Buleleng. (2015). *Laporan Triwulan Luas Areal dan Produksi Komoditas Perkebunan Kabupaten Buleleng Tahun 2015.*

Elachi, C., & Van Zyl, J. J. (2021). *Introduction to the physics and techniques of remote sensing*. John Wiley & Sons.

Green, E., Mumby, P., Edwards, A., & Clark, C. (2000). *Remote sensing: handbook for tropical coastal management*. United Nations Educational, Scientific and Cultural Organization (UNESCO).

Huete, A. R., & Glenn, E. P. (2011). Remote sensing of ecosystem structure and function. *Advances in Environmental Remote Sensing. Sensors, Algorithms, and Applications. CRC Press, Boca Raton, Florida, USA*, 291-320.

Lillesand, T., Kiefer, R. W., & Chipman, J. (2015). *Remote sensing and image interpretation*. John Wiley & Sons.

Limin, S. G., Oue, H., Sato, Y., & Budiasa, I. W. (2015). Partitioning rainfall into throughfall, stemflow, and interception loss in Clove (Syzygium aromaticum) plantation in upstream Saba River Basin, Bali. *Procedia Environmental Sciences*, *28*, 280-285. https://doi.org/10.1016/j.proenv.2015.07.036

Myeong, S., Nowak, D. J., & Duggin, M. J. (2006). A temporal analysis of urban forest carbon storage using remote sensing. *Remote Sensing of Environment*, *101*(2), 277-282. https://doi.org/10.1016/j.rse.2005.12.001

Ozdogan, M. (2010). The spatial distribution of crop types from MODIS data: Temporal unmixing using Independent Component Analysis. *Remote Sensing of Environment*, *114*(6), 1190-1204. https://doi.org/10.1016/j.rse.2010.01.006

Rees, W. G. (2013). *Physical principles of remote sensing*. Cambridge university press.

Roth, S. I., Leiterer, R., Volpi, M., Celio, E., Schaepman, M. E., & Joerg, P. C. (2019). Automated detection of individual clove trees for yield quantification in northeastern Madagascar based on multi-spectral satellite data. *Remote Sensing of Environment*, *221*, 144-156. https://doi.org/10.1016/j.rse.2018.11.009

Roy, D. P., Kovalskyy, V., Zhang, H. K., Vermote, E. F., Yan, L., Kumar, S. S., & Egorov, A. (2016). Characterization of Landsat-7 to Landsat-8 reflective wavelength and normalized difference vegetation index continuity. *Remote sensing of Environment*, *185*, 57-70. https://doi.org/10.1016/j.rse.2015.12.024

Santillan, J. R., & Makinano-Santillan, M. (2018). Analysis Of In-Situ Spectral Reflectance Of Sago And Other Palms: Implications For Their Detection In Optical Satellite Images. *ISPRS Annals of Photogrammetry, Remote Sensing & Spatial Information Sciences*, *4*(3).

Sims, D. A., & Gamon, J. A. (2002). Relationships between leaf pigment content and spectral reflectance across a wide range of species, leaf structures and developmental stages. *Remote sensing of environment*, *81*(2-3), 337-354. https://doi.org/10.1016/S0034-4257(02)00010-X

Sims, D. A., & Gamon, J. A. (2003). Estimation of vegetation water content and photosynthetic tissue area from spectral reflectance: a comparison of indices based on liquid water and chlorophyll absorption features. *Remote sensing of environment*, *84*(4), 526-537. https://doi.org/10.1016/S0034-4257(02)00151-7

Storey, J., Roy, D. P., Masek, J., Gascon, F., Dwyer, J., & Choate, M. (2016). A note on the temporary misregistration of Landsat-8 Operational Land Imager (OLI) and Sentinel-2 Multi Spectral Instrument (MSI) imagery. *Remote Sensing of Environment*, *186*, 121-122. https://doi.org/10.1016/j.rse.2016.08.025

Teixeira Pinto, C., Jing, X., & Leigh, L. (2020). Evaluation Analysis of Landsat Level-1 and Level-2 Data Products Using In Situ Measurements. *Remote Sensing*, *12*(16), 2597.

Vermote, E., Justice, C., Claverie, M., & Franch, B. (2016). Preliminary analysis of the performance of the Landsat 8/OLI land surface reflectance product. *Remote Sensing of Environment*, *185*, 46-56. https://doi.org/10.1016/j.rse.2016.04.008

Wang, T., Kou, X., Xiong, Y., Mou, P., Wu, J., & Ge, J. (2010). Temporal and spatial patterns of NDVI and their relationship to precipitation in the Loess Plateau of China. *International Journal of Remote Sensing*, *31*(7), 1943-1958.

Weng, Q. (2011). Remote sensing of vegetation with landsat imagery. In *Advances in Environmental Remote Sensing* (pp. 3-30). CRC Press..

Xie, Y., Sha, Z., & Yu, M. (2008). Remote sensing imagery in vegetation mapping: a review. *Journal of plant ecology*, *1*(1), 9-23.

Yuliara, I. M., MT, I., YULIARA, M., Kasmawan, I. G. A., & KASMAWAN, I. G. A. (2017). The Reflectance Spectral Characteristic of Cloves Vegetation Using Landsat 8 in Buleleng Bali. *Journal of Food Security and Agriculture*, *1*(1).

Yuliara, I. M., Ratini, N. N., Windarjoto, W., & Suandayani, N. K. T. (2020). Spectral reflectance and principal component analysis on the distribution of clove vegetation using Landsat 8. *International Journal of Physical Sciences and Engineering*, *4*(3), 27-37. https://doi.org/10.29332/ijpse.v4n3.611

Yuliara, I. M., Sutapa, G. N., & Kasmawan, G. A. (2018). Development and optimization of the ratio vegetation index on the visible and infrared spectrum. *International Journal of Physical Sciences and Engineering*, *2*(2), 101-110. https://doi.org/10.29332/ijpse.v2n2.172

Biography of Authors

	**I Made Yuliara** He lives at Jalan Kedondong No. 8 Denpasar, Bali, phone: 08123644116, he was born on July 18, 1964. Educational background : 1. Bachelor of Physics Program at Airlangga University in Surabaya, 1994 2. Master of Remote Sensing Program at Institute of Technology 10 November in Surabaya, 2000 *Email: imdyuliara@unud.ac.id*
	**Ni Nyoman Ratini** She lives at Jalan Lingkar Timur Unud Perumahan Panorama Jimbaran Blok B No. 21 Bukit Jimbaran, phone: 08123895890, she was born in April 1, 1967. Educational background : 1. Bachelor of Physics Program at Airlangga University in Surabaya, 1992 2. Master of Physics Science Program at Institute of Technology Bandung in Bandung, 2001 *Email: n_ratini@yahoo.com*
	**Gde Antha Kasmawan** He lives at Baha, Mengwi, Badung, Bali, phone: 081337314289, he was born on June 24, 1967. Educational background : 1. Bachelor of Physics Program at Airlangga University in Surabaya, 1994 2. Master of Physics Science Program at Institute of Technology Bandung in Bandung, 2001 *Email: gdeanthakas@yahoo.com*